Frustrated double ionization of atoms in strong laser fields

YINGBIN LI,[1] JINGKUN XU,[1] BENHAI YU,[1,3] AND XU WANG[2,4]

[1]*College of Physics and Electronic Engineering, Xinyang Normal University, Xinyang 464000, China*
[2]*Graduate School, China Academy of Engineering Physics, Beijing 100193, China*
[3]*hnyubenhai@163.com*
[4]*xwang@gscaep.ac.cn*

Abstract: With a three-dimensional classical ensemble method, we theoretically investigated frustrated double ionization (FDI) of atoms with different laser wavelengths. Our results show that FDI can be more efficiently generated with shorter wavelengths and lower laser intensities. With proper laser parameters more FDI events can be generated than normal double ionization events. The physical condition under which FDI events happen is identified and explained. The energy distribution of the FDI products - atomic ions in highly excited states - shows a sensitive wavelength dependency.

1. Introduction

The interaction of gas-phase atoms or molecules with strong laser fields has led to novel physical phenomena, such as high harmonic generation (HHG) [1–3], high-order above threshold ionization (HATI) [4–5], non-sequential double ionization (NSDI) [6–8], etc. These phenomena can be understood with a three-step recollision model [9–10]. In this model, an electron is first emitted via tunneling from the atom or molecule when the laser electric field becomes comparable to the binding Coulomb field. Then, the emitted electron is accelerated and driven back by the oscillating laser electric field, and recombines with the parent ion core to release high-energy photons, or collides elastically or inelastically with the parent ion core, leading to HATI or NSDI.

It has also been observed that a fraction of neutral atoms survive in the form of high-lying Rydberg states [11–13]. The mechanism for the creation of highly excited neutral atoms has attracted attention during the past years. Nubbemeyer *et al*. demonstrated that excited neutral atoms are formed through a frustrated tunneling ionization (FTI) process: the tunneled electron does not gain enough drift energy from the laser field and eventually is recaptured by the parent ion core [11]. The energy distribution of the resulting Rydberg states has been studied both theoretically and experimentally [14–16]. The ellipticity and pulse duration dependence of the yield of the exited neutral atoms has been explored [17–19]. It has also been shown that the FTI process is responsible for a zero-energy dip in the photoelectron energy spectrum of strong-field tunneling ionization [20].

For two-electron systems, the similar process is known as frustrated double ionization (FDI) [21–24]. Molecular FDI has been experimentally studied by measuring molecular fragments from Coulomb explosions [25] and theoretically simulated using quasiclassical models [26–28]. Very recently, atomic FDI has also been observed experimentally using three-body coincidence detections [29]. In an FDI process, two electrons are emitted during the laser pulse, but one of them is eventually recaptured, resulting in an excited ion, or an excited neutral atom plus an ion for a molecular case if the remaining molecular ion dissociates. A sample atomic FDI trajectory is illustrated in Fig. 1(a), with an NSDI trajectory shown in Fig. 1(b) for comparison. The evolution of individual electron energies for the two trajectories is shown in Figs. 1(c) and 1(d), respectively.
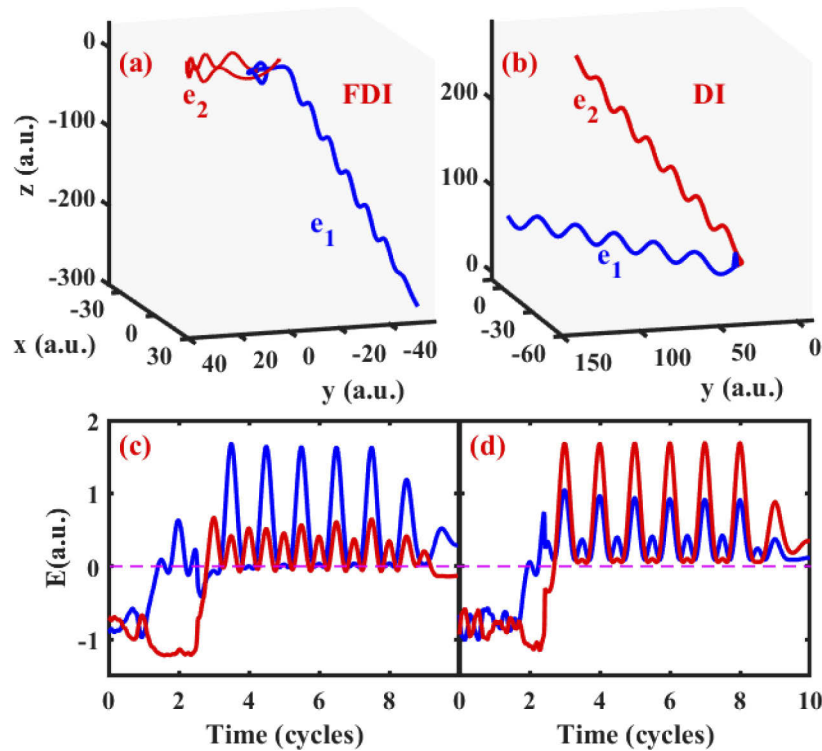
Fig. 1. (a) An example FDI trajectory. (b) An example NSDI trajectory. (c) The energy evolution of each electron for the trajectory shown in (a). (d) The energy evolution of each electron for the trajectory shown in (b).

Atomic FDI processes have been studied by Shomsky *et al.* [21] using a classical ensemble method and they pointed out that FDI is closely connected to a double ionization channel called recollision excitation with subsequent ionization (RESI). However, precise condition under which an FDI event can happen was not given. The goal of the current article is to give such a condition. We show that for an FDI event to happen, an electron must be emitted with an initial velocity that matches the laser vector potential at the time of emission. Therefore FDI is also closely related to the recently hot debated topic of ionization-exit velocity: the initial (longitudinal) velocity of the electron at the ionization exit [30–34].

The current article also emphasizes the wavelength dependency of FDI. Our results show that FDI clearly prefers shorter wavelengths and lower intensities. With proper laser parameters, more FDI events can be generated than normal double ionization events. Besides, the energy distribution of the FDI products – atomic ion in highly excited states – depends sensitively on wavelength. Therefore laser wavelength is a useful and efficient knob controlling the yield and the property of FDI.

2. Method

Accurate description of a two-active-electron atom in a strong laser field requires numerically solving the corresponding time-dependent Schrödinger equation. However, the computational load is very demanding if not impossible [35–38]. An alternative classical ensemble method was developed by Eberly and coworkers aiming at gaining insights into strong-field double ionization processes and explaining experimental data qualitatively [39–51]. The general idea is to mimic

the evolution of the quantum wavefunction using an ensemble of classically modeled atoms. The evolution of a two-active-electron atom in this model is governed by the Newton's equations of motion (atomic units are used unless stated otherwise)

$$d^2\mathbf{r}_i/dt^2 = -\nabla[V_{ne}(r_i) + V_{ee}(r_{12})] - \mathbf{E}(t), \qquad (1)$$

where the subscript $i = 1, 2$ is the electron label, $\mathbf{r}_i$ is the position of the i-th electron, $\mathbf{r}_{12}$ is the relative position of the two electrons, and $\mathbf{E}(t) = \hat{z}E_0 f(t)\sin(\omega t)$ is a linearly polarized laser electric field along the z axis. V_{ne} is the ion core-electron potential energy and V_{ee} is the electron-electron potential energy, and their forms will be given below. In the current article we use a trapezoidal pulse envelope function $f(t)$ with two cycles turning on, six cycles plateau, and two cycles turning off.

   The initial positions and momenta of the two electrons are randomly assigned such that they fulfill the energy constraint that the total energy equals to the negative sum of the first two ionization potentials of the target atom

$$E_{tot} = \left(\frac{p_1^2}{2} - \frac{2}{\sqrt{r_1^2 + a^2}}\right) + \left(\frac{p_2^2}{2} - \frac{2}{\sqrt{r_2^2 + a^2}}\right) + \frac{1}{\sqrt{r_{12}^2 + b^2}} = -(I_{p1} + I_{p2}) \qquad (2)$$

where $\mathbf{p}_i$ is the momentum of the i-th electron. I_{p1} and I_{p2} are the first and second ionization potential of the target atom, respectively. In the current article, we use argon as our target atom so the initial total energy is -1.59 a.u. Our conclusions and understandings, however, apply equally well to other atoms. In order to avoid unphysical autoionization and numerical singularity, soft-core Coulomb potentials have been adopted and the softening parameter a is set to be 1.5 a.u. and b to be 0.05 a.u. The system is allowed to evolve a sufficient long time (200 a.u.) without the laser field to obtain stable momentum and position distributions in the phase space. Once the initial positions and momenta are obtained, the laser pulse is turned on. We record the energy evolution of the two electrons every 0.01 laser cycles and identify a double ionization (DI) event if both electrons achieve positive energies at the end of the laser pulse. We identify an FDI event if both electrons achieve positive energies at some time during the laser pulse, and at the end of the pulse, one of the electrons is recaptured and has negative energy. The energy of each electron includes the kinetic energy, ion core-electron potential energy, and half of the electron-electron repulsion energy.

3. Numerical results and discussions

Figures 2(a)–2(c) displays the probabilities of FDI (red triangles) and DI (green squares) as a function of laser intensity for 400-nm, 800-nm and 1200-nm laser fields, respectively. One sees that for the three wavelengths, the probability curves of FDI increase rapidly at low intensities then slowly at high intensities. Especially in Fig. 2(c), the probability curve of FDI is close to saturation when the intensity is higher than about 1×10^{14} W/cm^2. In general, the probability curves of FDI display similar trends as the corresponding DI curves.

   Both electrons are emitted during the laser pulse, and whether one of them can be recaptured by the parent ion core at the end of pulse determines whether an FDI or a DI event happens. In this sense there is a competition between FDI and DI. For the 400-nm case as shown in Fig. 2(a), we can see a crossing between the DI and FDI probability curves around 9×10^{13} W/cm^2, below which FDI is more efficiently generated and above which DI is more efficient. For the 800-nm and 1200-nm cases, a similar crossing is not seen, and the probabilities of DI are always higher than those of FDI. In Fig. 2(d) the probability ratios between FDI and DI are plotted for the three wavelengths. We see that the ratios decrease with the increase of the laser wavelength, and also
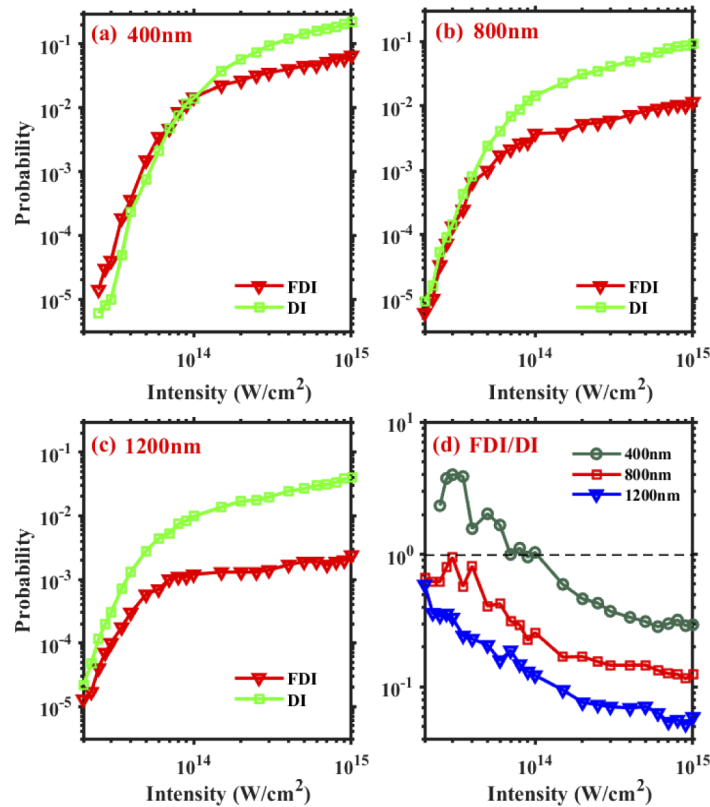
Fig. 2. Probabilities of FDI (red triangles) and DI (green squares) as a function of laser intensity for (a) 400-nm, (b) 800-nm, and (c) 1200-nm laser fields. (d) The ratio of yields between FDI and DI as a function of the laser intensity at the three wavelengths.

decrease with the increase of the laser intensity. That is, FDI prefers shorter wavelengths and lower intensities.

In order to understand the different microscopic electron dynamics, we trace back the history of the two-electron trajectories and find the recollision time (t_r) and the final ionization time (t_{i2}). The recollision time is defined as the instant of the closest approach of the two electrons after the first departure of one electron, and the final ionization time is defined as the instant when the energies of both electrons just become positive for the first time. Figure 3 shows the laser phase at final ionization versus that at recollision (both in laser cycles) for FDI (upper row) and for DI (lower row). The laser peak intensity is 5×10^{14} W/cm^2 and the laser wavelengths are 400 nm (left column), 800 nm (middle column) and 1200 nm (right column), respectively.

Different DI channels can be distinguished from the $t_{i2} - t_r$ phase diagrams. The diagonal populations correspond to the recollision impact ionization (RII) channel, for which the recollision is so prompt that the time difference between t_r and t_{i2} is small. The off-diagonal populations correspond to the RESI channel. The RESI contribution is estimated to be 88% for Fig. 3(d), 62% for Fig. 3(e), and 48% for Fig. 3(f).

For the 400-nm case, the population in the $t_{i2} - t_r$ phase diagram concentrates around two horizontal lines of $t_{i2} = 0.25$ or 0.75 cycles, for both FDI and DI [see Figs. 3(a) and 3(d)]. This implies that FDI and DI are both connected to the RESI mechanism: the bound electron cannot be promptly knocked out by the recolliding electron, and it has to wait until the next field maximum (0.25 or 0.75 cycles) to be pulled out by the laser field. This is consistent to the
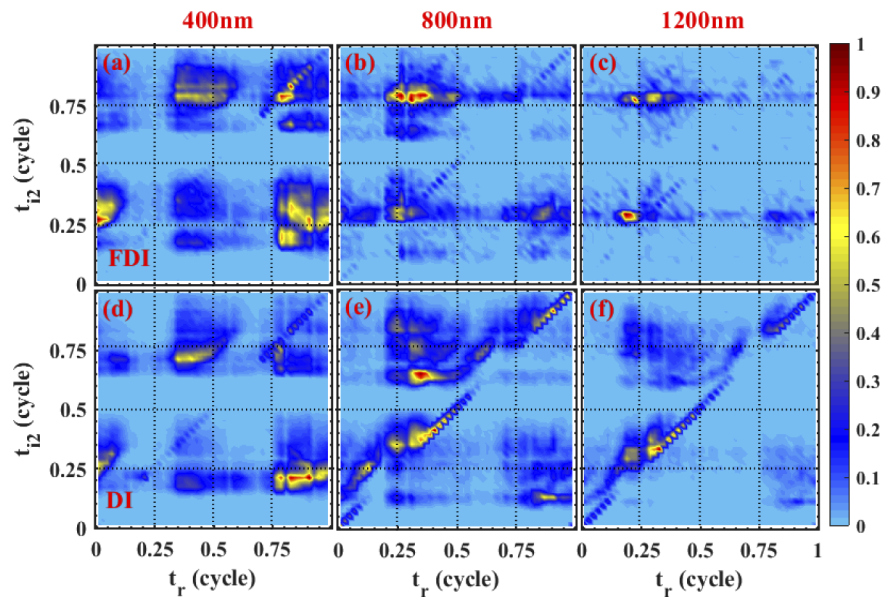
Fig. 3. Laser phase at final ionization time (t_{i2}) vs. laser phase at recollision time (t_r) (both in laser cycles). Upper row is for FDI and lower row is for DI. The laser wavelengths are 400 nm (a, d), 800 nm (b, e), and 1200 nm (c, f), respectively.

conclusion of Shomsky *et al.* [21]. The reason is that the maximal recollision energy ($3.17U_p$) is less than the binding energy of the second electron for 400 nm. Here, $Up = E_0^2/4\omega^2$ denotes the ponderomotive energy.
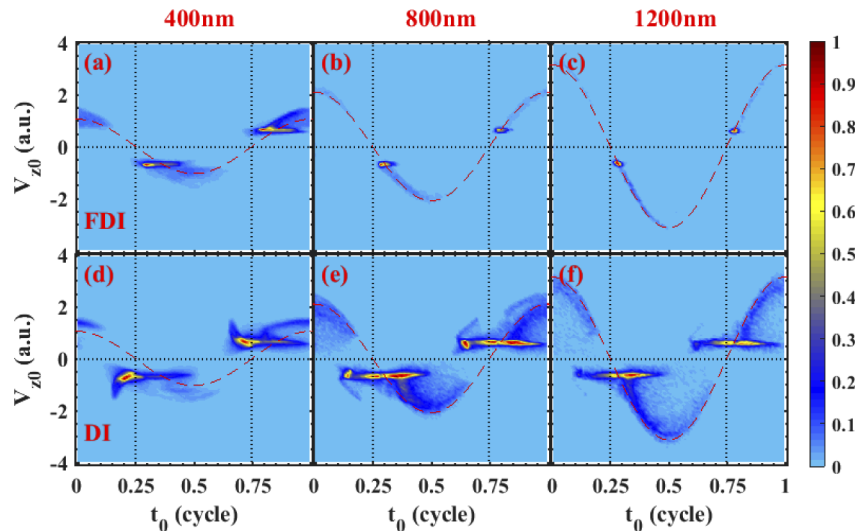

Fig. 4. Ionization-exit velocity along the laser polarization direction (V_{z0}) vs. ionization time (t_0) of the recaptured electron for successful FDI events (upper row). For normal DI events (lower row), V_{z0} and t_0 are for the second emitted electron. The laser wavelengths are 400 nm (left), 800 nm (middle) and 1200 nm (right), respectively. The red dashed curve in each panel shows the vector potential $A(t)$.

When the laser wavelength is increased to 800 nm and 1200 nm, the dominant part of the population switches gradually from horizontal to diagonal for DI [see Figs. 3(e) and 3(f)]. This is because the recollision energy is now larger than the binding energy of the second electron, and the mechanism of DI switches to RII. In contrast, for FDI, the population in the $t_{i2} - t_r$ phase diagram remains horizontal [see Figs. 3(b) and 3(c)]. This tells that the FDI mechanism prefers RESI channel, regardless of laser wavelengths.

Figure 4 shows the ionization-exit velocity (V_{z0}) along the laser polarization direction verses the ionization time (t_0) (in cycles) of the recaptured electron, for successful FDI events (upper row). For normal DI events, the ionization-exit velocity V_{z0} and the ionization time t_0 are for the second emitted electron. The red dashed curve in each panel shows the vector potential $A(t) = -\int_{-\infty}^{t} E(t)dt$. It is seen that for an FDI event to happen, an electron must be emitted with the right initial velocity. The initial velocity must be equal to (or very close to) the vector potential at the time of emission, so that the final velocity of the electron at the end of pulse, $P_z \approx V_{zo} - A(t_0)$ (neglecting Coulomb potentials after emission), is equal to (or very close to) zero.

A small mismatch between V_{z0} and $A(t_0)$ may be tolerated because the existence of the negative ion core-electron potential energy. That is, even the kinetic energy is not exactly zero, the total energy may still be negative. This tolerance is obviously wavelength dependent, as can also be seen from the distributions of Figs. 4(a), 4(b) and 4(c), where the population concentrates more and more tightly to the vector potential curve as the laser wavelength increases. This is because the shorter the wavelength, the shorter the electron quiver distance, the closer the electron to the ion core, and the more negative the ion core-electron potential energy.

Of course for an FDI event to happen, the electron must also be emitted with a near-zero transverse velocity (velocity perpendicular to the laser polarization direction). Otherwise the electron will fly away from the ion core in the transverse direction and cannot be recaptured.
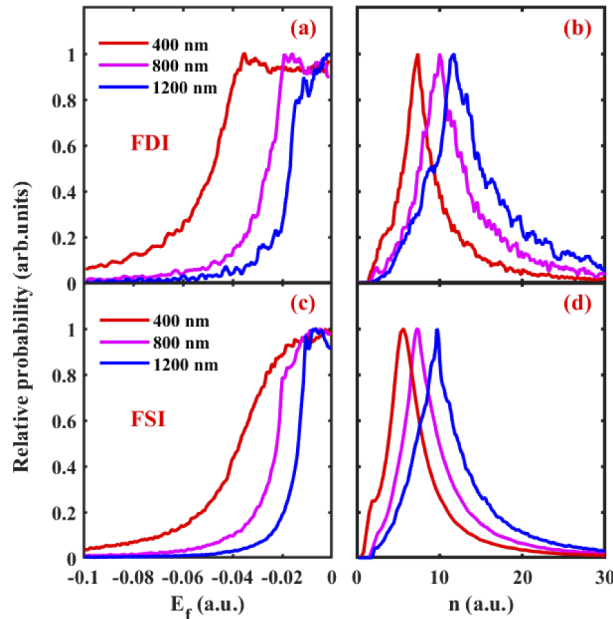

Fig. 5. (a) The final energy distribution of the recaptured electron in FDI events for the 400 nm, 800 nm, and 1200 nm lasers. (b) The effective principal quantum number distributions of the recaptured electron, for the same wavelengths. (c) and (d) the same as (a) and (b), but for the frustrated single ionization events.

Populations in Figs. 4(d), 4(e) and 4(f) along the vector potential curve correspond to nonzero initial transverse velocity.

The energy distributions of the recaptured electron at the end of pulse are shown in Fig. 5(a) for the three wavelengths. One sees that the energy increases as the wavelength increases, for the same reason as just explained above. One might also present the final energy distribution in terms of an effective principal quantum number, in order to have a better connection with Rydberg states, using the formula $n = \sqrt{-2/E_f}$. The distribution of this quantum number n is shown in Fig. 5(b). We see that for the three wavelengths, the peak of this principal quantum number distribution is at $n = 7$ (400 nm), $n = 10$ (800 nm), and $n = 11$ (1200 nm). So a longer wavelength will generate FDI events with higher Rydberg states, although the efficiency drops. Wavelength is thus a useful knob to control the FDI products and the resulting Rydberg state distributions.

Finally, for the purpose of connecting with existing results in the literature, we collect all the frustrated single ionization (FSI) events and plot the energy distributions as well as the effective principal quantum number distributions. The results are shown in Figs. 5(c) and 5(d). One sees that for the three wavelengths, the peaks of the principal quantum number distributions are around $n = 6 - 10$, consistent to results reported in the literature [11,52,53]. Obviously, the n distribution of FSI events is also sensitive to the laser wavelength, similar to FDI events.

4. Conclusion

Using a well-established classical ensemble method, we theoretically investigated FDI of atoms in strong laser fields. To be clearer for the readers, we first summarize the various mentioned physical processes as follows. In a strong laser field, an electron emitted from an atom may be driven back to recollide with its parent ion core. If this electron is recaptured, leaving the resultant neutral atom in an excited state, then this process is called FSI. If the recolliding electron kicks out a second electron promptly, then this process is called the RII channel of DI. If the recolliding electron only excites a second electron, and the second electron is later pulled out by the laser field, then this process is called the RESI channel of DI. If one of the two emitted electrons happens to be recaptured by the ion core, resulting in an excited singly charge ion, then this process is called FDI. FDI is understood to be closely related to the RESI channel.

We show that FDI prefers shorter wavelengths and lower intensities. With proper laser parameters, more FDI events can be generated than normal DI events. A precise condition of generating FDI events is given, that the initial electron velocity at the time of ionization must be equal (or very close) to the laser vector potential at the same time. Therefore FDI is also closely related to the currently hot debated topic of ionization-exit velocity of the electron.

We emphasize the importance of laser wavelength in generating and controlling FDI. The laser wavelength not only controls the yield but also the property of the FDI products - highly excited atomic ions. We show that the energy distribution of the excited atomic ions depends sensitively on laser wavelengths.

Disclosures

The authors declare that there are no conflicts of interest related to this article.

References

1. A. McPherson, G. Gibson, H. Jara, U. Johann, T. S. Luk, I. A. McIntyre, K. Boyer, and C. K. Rhodes, "Studies of multiphoton production of vacuum-ultraviolet radiation in the rare gases," J. Opt. Soc. Am. B **4**(4), 595–601 (1987).
2. F. Krausz and M. Ivanov, "Attosecond physics," Rev. Mod. Phys. **81**(1), 163–234 (2009).
3. J. Seres, E. Seres, A. J. Verhoef, G. Tempea, C. Streli, P. Wobrauschek, V. Yakovlev, A. Scrinzi, C. Spielmann, and F. Krausz, "Source of coherent kiloelectronvolt X-rays," Nature **433**(7026), 596 (2005).
4. G. G. Paulus, W. Nicklich, H. Xu, P. Lambropoulos, and H. Walther, "Plateau in above threshold ionization spectra," Phys. Rev. Lett. **72**(18), 2851–2854 (1994).
5. W. Becker, F. Grasbon, R. Kopold, D. B. Milošević, G. G. Paulus, and H. Walther, "Above-threshold ionization: From classical features to quantum effects," Adv. At., Mol., Opt. Phys. **48**, 35–98 (2002).
6. D. N. Fittinghoff, P. R. Bolton, B. Chang, and K. C. Kulander, "Observation of nonsequential double ionization of helium with optical tunneling," Phys. Rev. Lett. **69**(18), 2642–2645 (1992).
7. B. Walker, B. Sheehy, L. F. DiMauro, P. Agostini, K. J. Schafer, and K. C. Kulander, "Precision measurement of strong field double ionization of helium," Phys. Rev. Lett. **73**(9), 1227–1230 (1994).
8. A. Staudte, C. Ruiz, M. Schöffler, S. Schössler, D. Zeidler, T. Weber, M. Meckel, D. M. Villeneuve, P. B. Corkum, A. Becker, and R. Dörner, "Binary and recoil collisions in strong field double ionization of helium," Phys. Rev. Lett. **99**(26), 263002 (2007).
9. P. B. Corkum, "Plasma perspective on strong field multiphoton ionization," Phys. Rev. Lett. **71**(13), 1994–1997 (1993).
10. K. C. Kulander, K. J. Schafer, and J. L. Krause, "Dynamics of Short-Pulse Excitation, Ionization and Harmonic Conversion, " in *Super-Intense Laser-Atom Physics*, edited by B. Piraux, A. L'Huillier, and K. Rzazewski, eds. (Plenum, 1993) pp. 95–110.
11. T. Nubbemeyer, K. Gorling, A. Saenz, U. Eichmann, and W. Sandner, "Strong-field tunneling without Ionization," Phys. Rev. Lett. **101**(23), 233001 (2008).
12. B. Manschwetus, T. Nubbemeyer, K. Gorling, G. Steinmeyer, U. Eichmann, H. Rottke, and W. Sandner, "Strong laser field fragmentation of H-2: coulomb explosion without double ionization," Phys. Rev. Lett. **102**(11), 113002 (2009).
13. B. Ulrich, A. Vredenborg, A. Malakzadeh, M. Meckel, K. Cole, M. Smolarski, Z. Chang, T. Jahnke, and R. Dörner, "Double-ionization mechanisms of the argon dimer in intense laser fields," Phys. Rev. A **82**(1), 013412 (2010).
14. U. Eichmann, A. Saenz, S. Eilzer, T. Nubbemeyer, and W. Sandner, "Observing rydberg atoms to survive intense laser fields," Phys. Rev. Lett. **110**(20), 203002 (2013).
15. H. Zimmermann, J. Buller, S. Eilzer, and U. Eichmann, "Strong-field excitation of helium: bound state distribution and spin effects," Phys. Rev. Lett. **114**(12), 123003 (2015).
16. S. V. Popruzhenko, "Quantum theory of strong-field frustrated tunneling," J. Phys. B: At., Mol. Opt. Phys. **51**(1), 014002 (2018).
17. K. Huang, Q. Xia, and L. Fu, "Survival window for atomic tunneling ionization with elliptically polarized laser fields," Phys. Rev. A **87**(3), 033415 (2013).
18. L. Zhao, J. Dong, H. Lv, T. Yang, Y. Lian, M. Jin, H. Xu, D. Ding, S. Hu, and J. Chen, "Ellipticity dependence of neutral Rydberg excitation of atoms in strong laser fields," Phys. Rev. A **94**(5), 053403 (2016).
19. J. McKenna, S. Zeng, J. J. Hua, A. M. Sayler, M. Zohrabi, N. G. Johnson, B. Gaire, K. D. Carnes, B. D. Esry, and I. Ben-Itzhak, "Frustrated tunneling ionization during laser-induced D_2 fragmentation: Detection of excited metastable D* atoms," Phys. Rev. A **84**(4), 043425 (2011).
20. H. Liu, Y. Liu, L. Fu, G. Xin, D. Ye, J. Liu, X. T. He, Y. Yang, X. Liu, Y. Deng, C. Wu, and Q. Gong, "Low yield of near-zero-momentum electrons and partial atomic stabilization in strong-field tunneling ionization," Phys. Rev. Lett. **109**(9), 093001 (2012).
21. K. N. Shomsky, Z. S. Smith, and S. L. Haan, "Frustrated nonsequential double ionization: A classical model," Phys. Rev. A **79**(6), 061402 (2009).
22. A. M. Sayler, J. McKenna, B. Gaire, N. G. Kling, K. D. Carnes, and I. Ben-Itzhak, "Measurements of intense ultrafast laser-driven D^{3+} fragmentation dynamics," Phys. Rev. A **86**(3), 033425 (2012).
23. A. Chen, H. Price, A. Staudte, and A. Emmanouilidou, "Frustrated double ionization in two-electron triatomic molecules," Phys. Rev. A **94**(4), 043408 (2016).
24. W. Zhang, Z. Yu, X. Gong, J. Wang, P. Lu, H. Li, Q. Song, Q. Ji, K. Lin, J. Ma, H. Li, F. Sun, J. Qiang, H. Zeng, F. He, and J. Wu, "Visualizing and steering dissociative frustrated double ionization of hydrogen molecules," Phys. Rev. Lett. **119**(25), 253202 (2017).
25. T. Nubbemeyer, U. Eichmann, and W. Sandner, "Excited neutral atomic fragments in the strong-field dissociation of N_2 molecules," J. Phys. B **42**(13), 134010 (2009).
26. A. Vilà, G. P. Katsoulis, and A. Emmanouilidou, "Sub-cycle attosecond control in frustrated double ionization of molecules," J. Phys. B **52**(1), 015604 (2019).
27. A. Emmanouilidou, C. Lazarou, A. Staudte, and U. Eichmann, "Routes to formation of highly excited neutral atoms in the breakup of strongly driven H_2," Phys. Rev. A **85**(1), 011402 (2012).
28. G. P. Katsoulis, R. Sarkar, and A. Emmanouilidou, "Enhancing frustrated double ionization with no electronic correlation in triatomic molecules using counter-rotating two-color circular laser fields," preprint at http://www.arxiv.org/abs/1908.06262.

29. S. Larimian, S. Erattupuzha, A. Baltuška, M. Kitzler-Zeiler, and X. Xie, "Frustrated double ionization of argon atoms in strong laser fields," Phys. Rev. Research **2**(1), 013021 (2020).

30. A. N. Pfeiffer, C. Cirelli, A. S. Landsman, M. Smolarski, D. Dimitrovski, L. B. Madsen, and U. Keller, "Probing the longitudinal momentum spread of the electron wave packet at the tunnel exit," Phys. Rev. Lett. **109**(8), 083002 (2012).

31. X. Sun, M. Li, J. Yu, Y. Deng, Q. Gong, and Y. Liu, "Calibration of the initial longitudinal momentum spread of tunneling ionization," Phys. Rev. A **89**(4), 045402 (2014).

32. N. Camus, E. Yakaboylu, L. Fechner, M. Klaiber, M. Laux, Y. Mi, K. Z. Hatsagortsyan, T. Pfeifer, C. H. Keitel, and R. Moshammer, "Experimental evidence for quantum tunneling time," Phys. Rev. Lett. **119**(2), 023201 (2017).

33. J. Tian, X. Wang, and J. H. Eberly, "Numerical detector theory for the longitudinal momentum distribution of the electron in strong field ionization," Phys. Rev. Lett. **118**(21), 213201 (2017).

34. R. Xu, T. Li, and X. Wang, "Longitudinal momentum of the electron at the tunneling exit," Phys. Rev. A **98**(5), 053435 (2018).

35. J. Parker, K. T. Taylor, C. W. Clark, and S. Blodgett-Ford, "Intensity-field multiphoton ionization of a two-electron atom," J. Phys. B **29**(2), L33–L42 (1996).

36. J. Parker, B. J. S. Doherty, K. T. Taylor, K. D. Schultz, C. I. Blaga, and L. F. DiMauro, "High-energy cutoff in the spectrum of strong-field nonsequential double ionization," Phys. Rev. Lett. **96**(13), 133001 (2006).

37. B. I. Schneider, L. A. Collins, and S. X. Hu, "Parallel solver for the time-dependent linear and nonlinear Schrödinger equation," Phys. Rev. E **73**(3), 036708 (2006).

38. S. X. Hu, "Optimizing the FEDVR-TDCC code for exploring the quantum dynamics of two-electron systems in intense laser pulses," Phys. Rev. E **81**(5), 056705 (2010).

39. R. Panfili, J. H. Eberly, and S. L. Haan, "Comparing classical and quantum dynamics of strong-field double ionization," Opt. Express **8**(7), 431–435 (2001).

40. Y. B. Li, B. H. Yu, Q. B. Tang, X. Wang, D. Y. Hua, A. H. Tong, C. H. Jiang, G. X. Ge, Y. C. Li, and J. G. Wan, "Transition of recollision trajectories from linear to elliptical polarization," Opt. Express **24**(6), 6469–6479 (2016).

41. P. J. Ho, R. Panfili, S. L. Haan, and J. H. Eberly, "Nonsequential double ionization as a completely classical photoelectric effect," Phys. Rev. Lett. **94**(9), 093002 (2005).

42. S. L. Haan, J. S. Van Dyke, and Z. S. Smith, "Recollision excitation, electron correlation, and the production of high-momentum electrons in double ionization," Phys. Rev. Lett. **101**(11), 113001 (2008).

43. F. Mauger, C. Chandre, and T. Uzer, "Strong field double ionization: the phase space perspective," Phys. Rev. Lett. **102**(17), 173002 (2009).

44. X. Wang and J. H. Eberly, "Effects of elliptical polarization on strong-field short-pulse double ionization," Phys. Rev. Lett. **103**(10), 103007 (2009).

45. X. Wang and J. H. Eberly, "Elliptical polarization and probability of double ionization," Phys. Rev. Lett. **105**(8), 083001 (2010).

46. X. Wang, J. Tian, and J. H. Eberly, "Angular correlation in strong-field double ionization under circular polarization," Phys. Rev. Lett. **110**(7), 073001 (2013).

47. J. L. Chaloupka and D. D. Hickstein, "Dynamics of strong-field double ionization in two-color counterrotating fields," Phys. Rev. Lett. **116**(14), 143005 (2016).

48. S. L. Haan, L. Breen, A. Karim, and J. H. Eberly, "Recollision dynamics and time delay in strong-field double ionization," Opt. Express **15**(3), 767–778 (2007).

49. S. L. Haan, Z. S. Smith, K. N. Shomsky, and P. W. Plantinga, "Electron drift directions in strong-field double ionization of atoms," J. Phys. B **42**(13), 134009 (2009).

50. Y. B. Li, X. Wang, B. H. Yu, Q. B. Tang, G. H. Wang, and J. G. Wan, "Nonsequential double ionization with mid-infrared laser fields," Sci. Rep. **6**(1), 37413 (2016).

51. W. Beck, X. Liu, P. J. Ho, and J. H. Eberly, "Theories of photoelectron correlated in laser-driven multiple atomic ionization," Rev. Mod. Phys. **84**(3), 1011–1043 (2012).

52. N. I. Shvetsov-Shilovski, S. P. Goreslavski, S. V. Popruzhenko, and W. Becker, "Capture into Rydberg states and momentum distributions of ionized electrons," Laser Phys. **19**(8), 1550–1558 (2009).

53. H. Zimmermann, S. Patchkovskii, M. Ivanov, and U. Eichmann, "Unified Time and Frequency Picture of Ultrafast Atomic Excitation in Strong Laser Fields," Phys. Rev. Lett. **118**(1), 013003 (2017).